IAA-AAS-DyCoSS2-14-08-07
AAS 14-553

CHARGING STRATEGIES FOR ELECTROSTATIC CONTROL OF SPACECRAFT FORMATIONS

Leonard Felicetti* **and Giovanni B. Palmerini†**

Formation control by means of electrostatic forces, generating attractive or repulsive actions by charging the satellites' surfaces, has been recently proposed for high altitude orbits to precisely maintain the configuration without risk of plume impingement. This paper focus on electrostatic control and switching strategies for charge distribution in spacecraft formations, taking into account the limits on the power requirements. Two nonlinear global control approaches are presented and applied to two and three satellites' formations. Then, an optimized charge distribution process among the satellites is discussed and applied to the three spacecraft formation case. Numerical simulations are performed in order to evaluate the advantages and drawbacks of this configuration control technique.

INTRODUCTION

The use of electrostatic forces (Coulomb forces) has been recently proposed for formation acquisition, maintenance and reconfiguration[1]. This new concept of formation control is based on the idea of generating attractive or repulsive actions among spacecraft by charging the satellites' surfaces, in order to control their mutual distances.

Some theoretical and numerical studies were carried on by important space agencies (NASA[2] and ESA[3,4]) through their advanced concept teams, in order to analyze the system performances and needs. The results of such studies were encouraging because they showed the possibility of achieving high specific impulses with limited power requirements. A surprising result of the Coulomb interaction study was that the magnitude of the inter-spacecraft forces is comparable with - and may actually exceed - the one provided by micro-propulsion systems proposed for formation keeping. New missions involving two or more spacecraft flying in very strict formation are allowed, with very limited propellant consumption and low amount of required power. Applications which can benefit from this control technique can be optical interferometry missions like large field-of-view planetary detectors or distributed remote sensing system observing the Earth in the visible band from higher orbits (MEO and GEO) [5].

With respect to the classical formation control the most suitable advantages are[5]: (a) no risk of thruster plume impingement or contamination of neighboring spacecraft, which is especially important for optical payload, (b) high equivalent specific impulse, despite limited electrical power

* Postdoctoral Researcher, DIAEE Dipartimento di Ingegneria Astronautica Elettrica ed Energetica, Università di Roma "La Sapienza", via Salaria 851, 00138 Roma, Italy.
† Associate Professor, DIAEE Dipartimento di Ingegneria Astronautica Elettrica ed Energetica, Università di Roma "La Sapienza", via Salaria 851, 00138 Roma, Italy.

requirements and (c) very high precision in control. Classic chemical propulsion systems cannot provide so fine and continuous thrust. On the other hand, electric thrusters allow for strict formation position tolerances, but the generated ion fluxes pollute the environment in a way which is especially dangerous in case of optical payloads. Instead, the Coulomb force based control concept allows for continuous, fine-resolution maneuverability, which will greatly improve formation acquisition and maintenance maneuvers, because of the rapidity at which the Coulomb forces can be continuously varied[5].

A limit of the technique is represented by the effectiveness of the electrostatic action that is related to the Debye length parameter, quantifying the shielding effect generated by space plasma. As a result, electrostatic control seems better suitable for high altitude orbits.

All formations present an unstable behavior if controlled by means of electrostatic forces applied in an open-loop strategy. Therefore, a feedback law is needed to gain a suitable behavior. The extensive research effort by Schaub et al. produced significant advances on modelling and control formations of two[6,7,8], three[9,10,11] and more[12] spacecraft. These studies clearly demonstrated the possibility to acquire and to precisely maintain desired distances between spacecraft.

In the case of two spacecraft formation the strategy provides the value of the product of the charges to be commanded to the two spacecraft, and its square root is clearly the homogeneous and preferred solution for each individual charge. When the number of spacecraft belonging to the formation increases, the problem becomes more and more complicated. There is indeed a larger number of parameters, but also a richer set of constraints imposed by the desired geometric configuration of the formation – not necessarily easy to apply at the same time on the existing orbital dynamics. Feasible solutions different from the square root of the charge products are likely to appear, and the continuity in the required forces should not be given as granted. An additional, operational constraint to limit the variations in time of the currents to be induced on the platforms should be included to handle sudden variations in required forces. Overall, the switching law for the charging of different spacecraft becomes a far from trivial problem. This paper is then focused on the strategies to distribute the charges in formations involving three platforms, with the goal to attain the desired configuration in a fast and efficient way, and a constraint on the currents to be generated on the spacecraft surfaces, that have to be kept as low as possible. A preliminary selection of the equations to design the controller was performed in [11,12]. In this work a nonlinear global control strategy is computed before, giving as output three desired product charges which cannot always be satisfied together. The selection of what charge product must be followed is accomplished following the control computation.

Following material begins with the description of the governing equations of spacecraft charging (section 1) and of the formation dynamics forced by electrostatic actions (section 2). The overall control scheme adopted in this paper is presented in section 3, where also two different global control strategies (Lyapunov based and SDRE controls) are described. Then a selection criteria and the switching strategy for the case of three spacecraft formation are presented in section 4, while in section 5 optimal charge distribution laws are derived satisfying a part of the charge products obtained from the global controller The numerical results for both two- and three-spacecraft formations reported in the last section before the conclusions, even if preliminary, proof the interest of the proposed technique, suggesting an in depth analysis taking into account technological constraints.

SPACECRAFT CHARGING MODEL

The charging technology is currently used for controlling the spacecraft potential with respect to the surrounding plasma environment. Specific devices (as the plasma contactor used on the International Space Station[13] or ion and electron emitters used in electric propulsion[14]) are commonly used for neutralizing the electrostatic charge of the spacecraft with respect the neighbor environ-

ment, in order to avoid breakdowns which can damage on board electronic hardware. It is worth to notice that the space plasma, interacting with the spacecraft surfaces, naturally charges the spacecraft negatively[3]. The phenomenon depends upon the local plasma density of electrons/ions, the local temperature of electrons/ions and the reached spacecraft charge. The resulting spacecraft charge dynamics is the resultant of an equilibrium between fast electrons and slower ions fluxes from/to the spacecraft and the neighbor space plasma: if the spacecraft is charged with positive charges, it will attract electrons coming from the neighbor plasma, vice-versa a flux of positive ions from the plasma will occur if the spacecraft charge is negative [3]. The possibility to actively control the charge of the spacecraft with respect to the neighbor plasma potential was experimentally demonstrated by SCATHA[15] and ATS[16] missions. Hollow cathodes (emitting flows of electrons through electron guns) and ion thrusters (emitting positive charges to the space) are commonly used for this purpose[13,14].

These flows can be considered as positive (for electrons) or as negative (for ions) currents (i_i and i_e respectively) which modify the spacecraft charge status q_{sc} through the relation[3]

$$\frac{dq_{sc}}{dt} = i_t \tag{1}$$

where $i_t = i_i + i_e$ is the resulting electric current. In the following the currents will be considered as positive when the electrons go from the spacecraft to the external environment, and the natural charging due to the surrounding plasma will be neglected by assuming that currents produced by the actuators are higher than natural election/ion fluxes (the contribution of charging devices will be actually limited by the on board power and by the dimensions of the hollow cathodes/anodes). Under these hypotheses we can assume that the charging and discharging phases are ruled by the following relation:

$$i_{sc} = \begin{cases} +i_{s+} & \text{if } i_{rq} > i_{s+} \\ k_c i_{rq} & \text{if } i_{s-} < i_{rq} < i_{s+} \\ -i_{s-} & \text{if } i_{rq} < i_{s-} \end{cases} \tag{2}$$

where i_{rq} is the requested current (which will be calculated by a dedicated controller) and the i_{s+} and i_{s-} are saturation currents of the electron and ion emitters respectively.

The resulting spacecraft potential V_{sc} with respect to the surrounding environment can be evaluated as:

$$V_{sc} = \frac{q_{sc}}{C_{sc}} \tag{3}$$

where C_{sc} is the resulting electric capacitance of the external spacecraft surfaces.

In order to avoid breakdowns between the spacecraft and the outer plasma, a condition concerning the differences between the two potentials must be satisfied during all the electrostatic maneuvers. In particular, the resulting condition can be roughly written as $V_{sc} - V_{pl} < \Delta V_{br}$, where V_{pl} is the potential of the plasma and ΔV_{br} is the maximum admissible potential ensuring that no breakdown current occurs between spacecraft and plasma. In order to take into account this problem, a saturation limit on spacecraft charge is included by assuming the following relation:

$$q_{s-} \le q_{sc} \le q_{s+} \tag{4}$$

where q_{s-} and q_{s+} are the lower and upper limits of the spacecraft charges calculated by taking into account Eq.(3) and the breakdowns potential limits.

The required power and the total energy needed will be taken into account as indexes of the performance of the maneuvers. In particular the required power to charge the spacecraft can be computed by the following relation[1]:

$$P_{sc} = i_{sc} V_{sc} \tag{5}$$

and a estimation of the required energy can be obtained by the integration of Eq.(5), leading to:

$$E_{sc} = \int_{t_0}^{t_f} P_{sc} dt = \int_{t_0}^{t_f} i_{sc} V_{sc} dt \tag{6}$$

DYNAMICS OF CHARGED SATELLITE FORMATIONS

Let us consider a formation of N satellites in a circular orbit and let us associate a Local Vertical Local Horizontal (LVLH) reference frame whose origin is coincident with the center of mass of the formation F, as depicted in Figure 1.

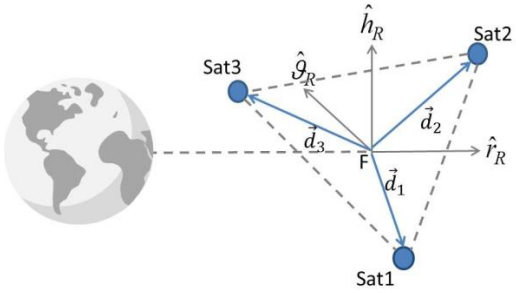

Figure 1. LVLH reference frame and $\vec{d}_i$ vector definition

The position of each spacecraft, with respect to the LVLH reference frame, is given by $\vec{d}_i$, whose components are aligned along the $\hat{r}_R$, $\hat{\vartheta}_R$ and $\hat{h}_R$ axes representing the radial, the in track and the orbit normal unit vectors respectively.

The dynamics of each satellite can be represented by the Clohessy-Wiltshire equations of motion[17]:

$$\ddot{\vec{d}}_i = 2n_0 \left(\hat{r}_R \hat{\vartheta}_R - \hat{\vartheta}_R \hat{r}_R \right) \cdot \dot{\vec{d}}_i + n_0^2 \left(3\hat{r}_R \hat{r}_R - \hat{h}_R \hat{h}_R \right) \cdot \vec{d}_i + \vec{f}_i \tag{7}$$

where $n_0 = \sqrt{\mu_\oplus / r_R^{\,3}}$ is the reference orbit mean motion, r_R is the reference orbit radius and $\vec{f}_i$ is the specific control force applied to the *i-th* spacecraft.

For electrostatic actuated spacecraft, the modeling of the control force is given by the following relation[4]:

$$\vec{f}_i = \frac{k_c}{m_i} \left(\sum_{\substack{j=1 \\ j \neq i}}^{N} \frac{q_i q_j}{d_{ij}^2} e^{-\frac{d_{ij}}{\lambda_d}} \hat{d}_{ij} \right) \tag{8}$$

where m_i is the spacecraft mass, q_i and q_j are respectively the charges of the *i-th* and the *j-th* spacecraft and λ_d is the Debye length, taking into account the shielding effects due to the space plasma. The vector $\vec{d}_{ij}$ (see Figure 2):

$$\vec{d}_{ij} = d_{ij} \hat{d}_{ij} = \vec{d}_i - \vec{d}_j \tag{9}$$

defines the distance between the spacecraft, with $\hat{d}_{ij}$ the relevant unit vector joining the *i-th* and *j-th* satellites.

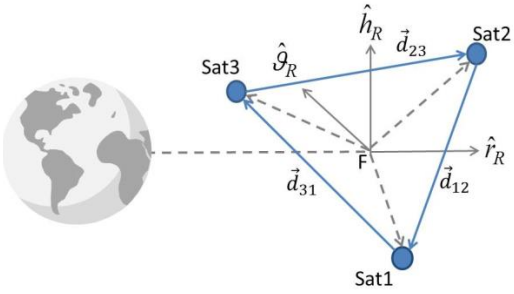

Figure 2. Distances among the spacecraft

Note that the specific forces defined by Eq.(8) are internal ones and cannot produce variations in the center of mass of the formation: only changes of relative position among spacecraft are possible by using electrostatic forces.

Equation (7) can be rearranged by taking into account Eq.(9) and considering all the possible spacecraft pairs in the formation. The resulting equations are representative of the dynamics of the $N(N-1)/2$ virtual links, connecting all the spacecraft of the formation, and can be written as:

$$\ddot{\vec{d}}_{ij} = 2n_0\left(\hat{r}_R\hat{\vartheta}_R - \hat{\vartheta}_R\hat{r}_R\right)\cdot\dot{\vec{d}}_{ij} + n_0^2\left(3\hat{r}_R\hat{r}_R - \hat{h}_R\hat{h}_R\right)\cdot\vec{d}_{ij} +$$

$$+k_c\left[\left(\frac{1}{m_i}+\frac{1}{m_j}\right)\frac{q_iq_j}{d_{ij}^2}e^{-\frac{d_{ij}}{\lambda_d}}\hat{d}_{ij} + \sum_{\substack{k=1\\k\neq i,j}}^{N}\left(\frac{1}{m_i}\frac{q_iq_k}{d_{ik}^2}e^{-\frac{d_{ik}}{\lambda_d}}\hat{d}_{ik} - \frac{1}{m_j}\frac{q_jq_k}{d_{jk}^2}e^{-\frac{d_{jk}}{\lambda_d}}\hat{d}_{jk}\right)\right] \tag{10}$$

The forces ruling the dynamics of each virtual link[18,19] can be divided between the "internal" to the link (electrostatic action between the *i-th* and *j-th* spacecraft) and the external ones, which involve a spacecraft of the selected pair and another spacecraft in the formation. Figure 3 shows the virtual link between the *1st* and the *2nd* spacecraft: the internal action (in green) acts only along the joining direction between the two spacecraft, producing a variation of the length of the virtual link. On the other hand the "external" forces (in red) can also produce a rotation or a translation of the virtual link by their components normal to the virtual link direction.

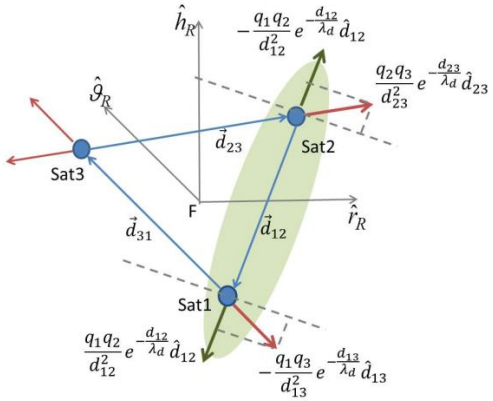

Figure 3. Electrostatic forces acting to the virtual link joining Sat 1 and Sat 2

In fact we can be project Eq.(10) along the $\hat{d}_{ij}$ direction, the only one which the electrostatic force can act on, to obtain the following scalar equation of motion representing the axial dynamics of a virtual link connecting the *i-th* spacecraft with the *j-th* spacecraft:

$$\ddot{d}_{ij} = n_0^2 d_{ij}\left[3\left(\hat{d}_{ij}\cdot\hat{r}_R\right)^2 - \left(\hat{d}_{ij}\cdot\hat{h}_R\right)^2\right] + \\ +k_c\left[\left(\frac{1}{m_i}+\frac{1}{m_j}\right)\frac{Q_{ij}}{d_{ij}^2}e^{-\frac{d_{ij}}{\lambda_d}} + \sum_{\substack{k=1\\k\neq i,j}}^{N}\left(\frac{1}{m_i}\frac{Q_{ik}}{d_{ik}^2}e^{-\frac{d_{ik}}{\lambda_d}}\left(\hat{d}_{ik}\cdot\hat{d}_{ij}\right) - \frac{1}{m_j}\frac{Q_{jk}}{d_{jk}^2}e^{-\frac{d_{jk}}{\lambda_d}}\left(\hat{d}_{jk}\cdot\hat{d}_{ij}\right)\right)\right] \tag{11}$$

where $Q_{ij} = q_i q_j$ is the product between two satellite charges.

The $N(N-1)/2$ equations of motion, resulting by iteration of Eq.(11), can be represented in the state space form as follows[20]:

$$\dot{\mathrm{X}} = \mathbf{A}(\mathrm{X})\,\mathrm{X} + \mathbf{B}(\mathrm{X})\,\mathrm{U} \tag{12}$$

with the state vector is defined as:

$$\mathrm{X} = \left[d_{12} \quad \cdots \quad d_{ij} \quad \cdots \quad d_{N-1,N}\ \dot{d}_{12} \quad \cdots \quad \dot{d}_{ij} \quad \cdots \quad \dot{d}_{N-1,N}\right]^T = \left[\mathrm{X}_d^T \quad \dot{\mathrm{X}}_d^T\right]^T \tag{13}$$

The plant matrix and the control distribution matrix can be detailed as:

$$\mathbf{A}(\mathrm{X}) = \begin{bmatrix} 0 & \mathbf{E} \\ \hat{\mathbf{A}}(\mathrm{X}) & 0 \end{bmatrix}; \qquad \mathbf{B}(\mathrm{X}) = \begin{bmatrix} 0 \\ \hat{\mathbf{B}}(\mathrm{X}) \end{bmatrix} \tag{14}$$

where the term of the sub-matrix $\hat{\mathbf{A}}(\mathrm{X})$ and of the sub-matrix $\hat{\mathbf{B}}(\mathrm{X})$ are directly obtained by taking into account Eq.(11), and $\mathbf{E}$ is the identity matrix. Finally, the control vector includes all the charge products:

$$U = \left[Q_{12} \quad \cdots \quad Q_{ij} \quad \cdots \quad Q_{N-1,N}\right]^T \tag{15}$$

FORMATION CONTROL STRATEGIES BY MEANS OF ELECTROSTATIC FORCES

One of the most peculiar aspects of the system of equation of motion in Eq.(11) is that the control actions depend on the product of the charges between two interacting spacecraft and not on their individual values. It is also clear that it would be impossible to act on a single spacecraft without affecting the others: a global guidance and control strategy is therefore the preferred option with respect to platform's individual guidance.

The analysis performed in the following is based on the architecture illustrated in Figure 4.The system's dynamics is represented by the Clohessy-Wiltshire equations of motion with the electrostatic forces (Eqs. (7)-(8)) and by an additional equation for each spacecraft of the formation describing the charge dynamics (Eq.(1)), with the relevant saturation limits on the currents (Eq.(2)) and the maximum and minimum allowable charges (Eq.(4)). The controller takes into account only the range and range rates among the spacecraft and, by means of the reduced set of equations of motion expressed by Eq.(12), computes the charge products needed to appropriately maneuver the spacecraft. The charge distribution function takes into account these products and selects which one among them must be implemented first, avoiding impossible control realizations. The selection process is continuously reconsidered in order to track the evolution of the formation and to give the priority to larger errors with respect to the desired configuration. The charge distribution provides as output the desired charges to each spacecraft.

A low level controller, acting on each spacecraft, takes the desired charge value and the actual charge status of the satellite and computes the required current. The charging actuators will track the current commanded by the charge controllers and produce the ion or electron fluxes the charges and the electrostatic forces to accomplish the maneuver.

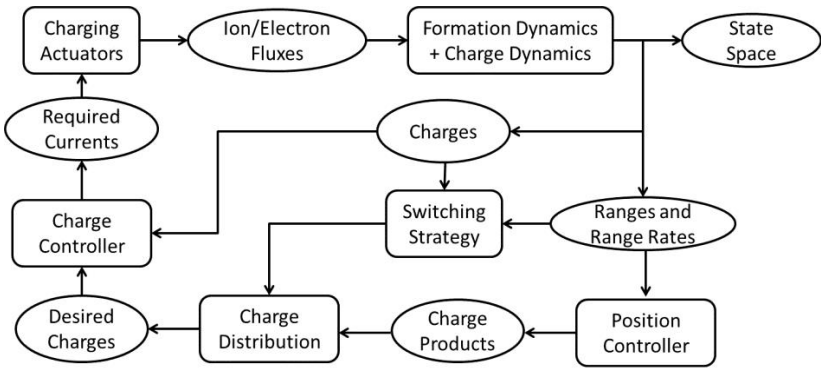

Figure 4. Architecture of the control strategy

Due to the highly non-linear dynamics which characterize the system, two non-linear formation control strategies will be investigated in the following. Specifically a Lyapunov based control scheme and the SDRE technique are considered. The two global control strategies will be described first, them a switching strategy will be presented for the three spacecraft formation case.

Lyapunov based control strategy

This control strategy, which can be applied to the system of equation of motion represented by the Eq.(11), is based on the definition of the following Lyapunov function[9,10,11,21]:

$$L = \sum_{i=1}^{N} \sum_{\substack{j=1 \\ j \neq i}}^{N} \left[\frac{1}{2} k_{ij}^{p} \left(d_{ij} - d_{ij}^{des} \right)^2 + \frac{1}{2} \dot{d}_{ij}^2 \right] \geq 0 \tag{16}$$

which is positive semi-definite and vanishes when the desired configuration is attained. Deriving Eq.(12) with respect to time offers

$$\dot{L} = \sum_{i=1}^{N} \sum_{\substack{j=1 \\ j \neq i}}^{N} \dot{d}_{ij} \left[k_{ij}^{p} \left(d_{ij} - d_{ij}^{des} \right) + \ddot{d}_{ij} \right] \tag{17}$$

to be negative semi-definite in order to ensure the asymptotic stability of the system. It is possible to substitute Eq.(11) leading to the following expression:

$$\begin{aligned} \dot{L} = \sum_{i=1}^{N} \sum_{\substack{j=1 \\ j \neq i}}^{N} \dot{d}_{ij} \left\{ k_{ij}^{p} \left(d_{ij} - d_{ij}^{des} \right) + n_0^2 d_{ij} \left[3 \left(\hat{d}_{ij} \cdot \hat{r}_R \right)^2 - \left(\hat{d}_{ij} \cdot \hat{h}_R \right)^2 \right] + k_c \left(\frac{1}{m_i} + \frac{1}{m_j} \right) \frac{Q_{ij}}{d_{ij}^2} e^{-\frac{d_{ij}}{\lambda_d}} + \right. \\ \left. + k_c \left[\sum_{\substack{k=1 \\ k \neq i,j}}^{N} \left(\frac{1}{m_i} \frac{Q_{ik}}{d_{ik}^2} e^{-\frac{d_{ik}}{\lambda_d}} \left(\hat{d}_{ik} \cdot \hat{d}_{ij} \right) - \frac{1}{m_j} \frac{Q_{jk}}{d_{jk}^2} e^{-\frac{d_{jk}}{\lambda_d}} \left(\hat{d}_{jk} \cdot \hat{d}_{ij} \right) \right) \right] \right\} \end{aligned} \tag{18}$$

The stability is granted by means of the position:

$$\dot{L} = -\sum_{i=1}^{N} \sum_{\substack{j=1 \\ j \neq i}}^{N} k_{ij}^{d} \dot{d}_{ij}^2 \tag{19}$$

which provides the following condition for each (*i-th, j-th*) couple of spacecraft:

$$k_{ij}^{p}\left(d_{ij}-d_{ij}^{des}\right)+k_{ij}^{d}\dot{d}_{ij}+n_0^2 d_{ij}^{5}\left[3\left(\hat{d}_{ij}\cdot\hat{r}_R\right)^2-\left(\hat{d}_{ij}\cdot\hat{h}_R\right)^2\right]+k_c\left(\frac{1}{m_i}+\frac{1}{m_j}\right)\frac{Q_{ij}}{d_{ij}^2}e^{-\frac{d_{ij}}{\lambda_d}}+$$
$$+k_c\left[\sum_{\substack{k=1\\k\neq i,j}}^{N}\left(\frac{1}{m_i}\frac{Q_{ik}}{d_{ik}^2}e^{-\frac{d_{ik}}{\lambda_d}}\left(\hat{d}_{ik}\cdot\hat{d}_{ij}\right)-\frac{1}{m_j}\frac{Q_{jk}}{d_{jk}^2}e^{-\frac{d_{jk}}{\lambda_d}}\left(\hat{d}_{jk}\cdot\hat{d}_{ij}\right)\right)\right]=0 \tag{20}$$

The set of Eq.(20) iterated for all the $N(N-1)/2$ pairs in the formation can be usefully recollected the following matrix expression:

$$\mathbf{K}_P\left(\mathrm{X}_d-\mathrm{X}_d^{des}\right)+\mathbf{K}_D\left(\dot{\mathrm{X}}_d-\dot{\mathrm{X}}_d^{des}\right)+\hat{\mathbf{A}}(\mathrm{X})\mathrm{X}_d+\hat{\mathbf{B}}(\mathrm{X})\,\mathrm{U}=0 \tag{21}$$

where $\mathbf{K}_P$ and $\mathbf{K}_D$ is the gain matrix containing the k_{ij}^{p} and k_{ij}^{d} in their diagonals.

Starting from the Eq.(21), the resulting control action reads as, if the matrix $\hat{\mathbf{B}}(\mathrm{X})$ can be inverted:

$$\mathrm{U}=-\hat{\mathbf{B}}(\mathrm{X})^{-1}\left[\mathbf{K}_P\left(\mathrm{X}_d-\mathrm{X}_d^{des}\right)+\mathbf{K}_D\left(\dot{\mathrm{X}}_d-\dot{\mathrm{X}}_d^{des}\right)+\hat{\mathbf{A}}(\mathrm{X})\mathrm{X}_d\right] \tag{22}$$

It is worth to notice that Eq.(22) contains feedback terms. The stability of such control scheme will be proved by numerical simulations in next sections. In that section, it will be also shown that this control strategy cannot cancel the steady state errors, while ensuring the stability of the system. In order to correct this problem, an integrative term is added to Eq.(22), leading to the following control strategy:

$$\mathrm{U}=-\hat{\mathbf{B}}(\mathrm{X})^{-1}\left[\mathbf{K}_I\int_{t_0}^{t}\left(\mathrm{X}_d-\mathrm{X}_d^{des}\right)dt+\mathbf{K}_P\left(\mathrm{X}_d-\mathrm{X}_d^{des}\right)+\mathbf{K}_D\left(\dot{\mathrm{X}}_d-\dot{\mathrm{X}}_d^{des}\right)+\hat{\mathbf{A}}(\mathrm{X})\mathrm{X}_d\right] \tag{23}$$

where the matrix $\mathbf{K}_I$ is diagonal and contains the gains related to the integral terms.

State dependent Riccati equation based control strategies

A different, suitable methodology of control is based on the minimization of the following cost function:

$$J=\int_{t_0}^{\infty}\left[\left(\mathrm{X}-\mathrm{X}^{des}\right)^T\mathbf{Q}(\mathrm{X})\left(\mathrm{X}-\mathrm{X}^{des}\right)+\mathrm{U}^T\mathbf{R}(\mathrm{X})\,\mathrm{U}\right]dt \tag{24}$$

where $\mathbf{Q}(\mathrm{X})$ is the matrix weighting the reachability of the desired state of the system and $\mathbf{R}(\mathrm{X})$ is the matrix weighting the control effort.

The solution of the optimization problem is granted if the system is linear, which is not the current case as all the matrices are state dependent. Recent advances in control research led to the development of the so called *"state dependent Riccati equation"* approach[22,23,24], identifying a sub-optimal solution of the problem provided that the system of equations of motion could be written in a *"state dependent coefficient form"* (SDC form). Eq.(12) clearly satisfies this requirement, therefore leading to the following control law:

$$\mathrm{U}=-\mathbf{R}^{-1}\mathbf{B}(\mathrm{X})^T\mathbf{P}(\mathrm{X})\left(\mathrm{X}-\mathrm{X}^{des}\right) \tag{25}$$

where the $\mathbf{P}(\mathrm{X})$ matrix is the solution of the *"time variable state dependent Riccati equation"*:

$$\dot{\mathbf{P}}(\mathrm{X})=\mathbf{P}(\mathrm{X})\mathbf{A}(\mathrm{X})+\mathbf{A}(\mathrm{X})^{\mathbf{T}}\mathbf{P}(\mathrm{X})-\mathbf{P}(\mathrm{X})\mathbf{B}(\mathrm{X})\mathbf{R}^{-1}\mathbf{B}(\mathrm{X})^{\mathbf{T}}\mathbf{P}(\mathrm{X})+\mathbf{Q} \tag{26}$$

to be solved iteratively by using the Taylor series method[23]. the solution $\mathbf{P}(\mathrm{X})$ of Eq.(22) is found as sum of *n* matrices $\left(\mathbf{P}_0(\mathrm{X}),\mathbf{P}_1(\mathrm{X}),\ldots\mathbf{P}_n(\mathrm{X})\right)$, which can be calculated by the following procedure[25]:

- to solve the algebraic Riccati equation by using the state depending matrices of the system dynamics:

$$\mathbf{P}_0(\mathrm{X})\mathbf{A}(\mathrm{X}) + \mathbf{A}(\mathrm{X})^{\mathrm{T}}\mathbf{P}_0(\mathrm{X}) - \mathbf{P}_0(\mathrm{X})\mathbf{B}(\mathrm{X})\mathbf{R}^{-1}\mathbf{B}(\mathrm{X})^{\mathrm{T}}\mathbf{P}_0(\mathrm{X}) + \mathbf{Q} = 0 \tag{27}$$

- to refine the solution by solving the associated algebraic Lyapunov equation for the first order solution:

$$\begin{aligned}\mathbf{P}_1(\mathrm{X})\left(\mathbf{A}(\mathrm{X}) - \mathbf{B}(\mathrm{X})\mathbf{R}^{-1}\mathbf{B}(\mathrm{X})^{\mathrm{T}}\mathbf{P}_0(\mathrm{X})\right) + \left(\mathbf{A}(\mathrm{X}) - \mathbf{B}(\mathrm{X})\mathbf{R}^{-1}\mathbf{B}(\mathrm{X})^{\mathrm{T}}\mathbf{P}_0(\mathrm{X})\right)^{\mathrm{T}}\mathbf{P}_1(\mathrm{X}) + \\ + \mathbf{P}_0(\mathrm{X})\Delta\mathbf{A}(\mathrm{X}) + \Delta\mathbf{A}(\mathrm{X})\mathbf{P}_0(\mathrm{X}) = 0\end{aligned} \tag{28}$$

- to solve the *n*-th order associated algebraic Lyapunov equation until the convergence of the solution:

$$\begin{aligned}\mathbf{P}_n(\mathrm{X})\left(\mathbf{A}(\mathrm{X}) - \mathbf{B}(\mathrm{X})\mathbf{R}^{-1}\mathbf{B}(\mathrm{X})^{\mathrm{T}}\mathbf{P}_0(\mathrm{X})\right) + \left(\mathbf{A}(\mathrm{X}) - \mathbf{B}(\mathrm{X})\mathbf{R}^{-1}\mathbf{B}(\mathrm{X})^{\mathrm{T}}\mathbf{P}_0(\mathrm{X})\right)^{\mathrm{T}}\mathbf{P}_n(\mathrm{X}) + \\ + \mathbf{P}_{n-1}(\mathrm{X})\Delta\mathbf{A}(\mathrm{X}) + \Delta\mathbf{A}(\mathrm{X})^{\mathrm{T}}\mathbf{P}_{n-1}(\mathrm{X}) - \sum_{j=1}^{n-1}\mathbf{P}_j(\mathrm{X})\mathbf{B}(\mathrm{X})\mathbf{R}^{-1}\mathbf{B}(\mathrm{X})^{\mathrm{T}}\mathbf{P}_{n-j}(\mathrm{X}) = 0\end{aligned} \tag{29}$$

The resulting SDRE control can be finally found as follows:

$$\mathrm{U}(\mathrm{X}) = -\mathbf{R}^{-1}\mathbf{B}(\mathrm{X})^{T}\sum_{n=0}^{N}\mathbf{P}_n(\mathrm{X})\left(\mathrm{X} - \mathrm{X}^{des}\right) \tag{30}$$

SWITCHING STRATEGIES FOR THREE SPACECRAFT FORMATIONS

The global strategy returns as output the products Q_{ij} among the spacecraft charges required to perform the maneuvers and does not solve completely the guidance problem. A charge distribution law is necessary to uniquely identify a charge value q_i, which satisfies the product charges Q_{ij} obtained by the higher level controller, solves for the possible ambiguities on distributing the charges, and avoids not implementable or destabilizing cases, with the last issues arising when the number of the spacecraft involved is higher than two. Let us make an example by using three spacecraft labeled as *i*, *j*, *k*, and forming an equilateral triangle as depicted in Figure 5.

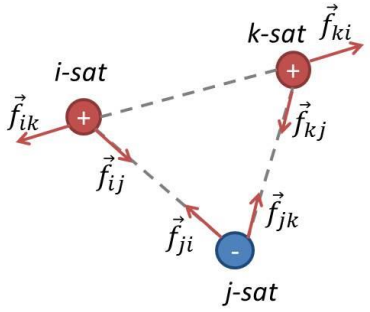

Figure 5. Three spacecraft formation dimension reduction

A simultaneous reduction of the sides of the triangle is not physically implementable. Indeed, if we suppose the sign of the charge of the spacecraft *i* as positive, the second satellite (*j*) will have a negative charge, and requires the positive sign of the third spacecraft (*k*) to reduce the two sides ending in *j*. However, the first and the third satellite charges ends up to have the very same sign, producing an increase of the distance between them. The considered controllers do not take into account this impossibility and provides as output a vector including three negative products. The problem can be solved by selecting only two of the three charge products as driving parameters

and by violating the remaining constraint[9]. Accordingly, the selected links will reduce their length but the remaining one will probably increase it. In order to assure a global convergence to the desired shape, the selection of the governing charge products must change periodically. Denoting as Δt_{sw} the switching period, an evaluation of cost functions at times $\left(t_{sw} = t_0 + m\Delta t_{sw} \quad m = 1,2...\right)$ will be required to iterate the selection of the active constraints. Specifically, the differences between actual and desired distances among the spacecraft can be adopted as selection criteria. The cost functions will conveniently read as:

$$E_{ij} = \frac{1}{2}\left(d_{ij} - d_{ij}^{des}\right)^2 \qquad E_{jk} = \frac{1}{2}\left(d_{jk} - d_{jk}^{des}\right)^2 \qquad E_{ki} = \frac{1}{2}\left(d_{ki} - d_{ki}^{des}\right)^2 \tag{31}$$

and the link to exclude will be the one offering the minimum value of the functions in Eq.(31). The remaining two links will drive the charge distribution algorithm with their associated charge products which will be enforced (hard constraints) during the charge distribution process.

OPTIMAL CHARGE DISTRIBUTION TO THE SPACECRAFT

Both the previous control approaches provide as output the charge products, but they do not give any information about the distribution of these charges to the spacecraft. Different distribution strategies have been studied in the past, satisfying different requirements. One of the most common requirements is the minimization of the spacecraft charge, in order to avoid breakdowns with the outer space plasma. This problem can be seen as a constrained optimization one[26], which can be analytically solved only in some simpler cases. In the following the cases of two and three spacecraft formation will be analyzed in detail. The two spacecraft distribution problem is discussed and solved first. However, the distribution problem becomes more complicates if the formation has three or more spacecraft: a general solution is not available, and a reduced optimality problem, respecting only two (out of three) charge product constraints will be therefore presented.

Two spacecraft optimal charge distribution

Given the charge product Q_{ij} between two spacecraft, the condition of minimum charge distribution can be obtained analytically by minimizing the following cost index:

$$V = \frac{1}{2}q_i^2 + \frac{1}{2}q_j^2 \tag{32}$$

subject to the product charge constraint obtained from the controller:

$$Q_{ij} - q_i q_j = 0 \tag{33}$$

By introducing the Lagrange multiplier λ_{ij}, it is possible to write the following Hamiltonian function:

$$H = \frac{1}{2}q_i^2 + \frac{1}{2}q_j^2 + \lambda_{ij}\left[Q_{ij} - q_i q_j\right] \tag{34}$$

The necessary condition for assuring the optimal choice of the charges can be written as follows:

$$\frac{\partial H}{\partial q_i} = q_i - \lambda_{ij} q_j = 0 \qquad \frac{\partial H}{\partial q_j} = q_j - \lambda_{ij} q_i = 0 \qquad \frac{\partial H}{\partial \lambda_{ij}} = Q_{ij} - q_i q_j = 0 \tag{35}$$

This system of equations can be solved analytically by evaluating λ_{ij} from the first equation and substituting it, together with the third equation, into the second one, as:

$$\lambda_{ij} = \frac{q_i}{q_j} \qquad q_j = \frac{Q_{ij}}{q_i} \qquad \left(q_i^2 + Q_{ij}\right)\left(q_i^2 - Q_{ij}\right) = 0 \tag{36}$$

Concerning the solution of Eq.(36), the driving parameter is the product Q_{ij} which can assume either positive or negative values. In both the cases the rightmost relation in Eq. (36) has two real and two imaginary roots. Real values are clearly the only suitable ones for the spacecraft charges, leading to two possible sets:

$$\begin{aligned} &a) \quad q_i = \sqrt{|Q_{ij}|} \qquad q_j = \frac{Q_{ij}}{\sqrt{|Q_{ij}|}} = sign(Q_{ij})\sqrt{|Q_{ij}|} \qquad \lambda_{ij} = sign(Q_{ij}) \\ &b) \quad q_i = -\sqrt{|Q_{ij}|} \quad q_j = -\frac{Q_{ij}}{\sqrt{|Q_{ij}|}} = -sign(Q_{ij})\sqrt{|Q_{ij}|} \quad \lambda_{ij} = sign(Q_{ij}) \end{aligned} \tag{37}$$

where $|Q_{ij}|$ represents the absolute value of Q_{ij} and $sign(Q_{ij})$ assumes as output $+1$ if $Q_{ij} > 0$ and -1 if $Q_{ij} < 0$. The indetermination between the two sets is due to the selection of which satellite must be charged positively or negatively when an attractive force is required $(Q_{ij} < 0)$, or whether both satellites must have positive or negative charges when a repulsive force is needed $(Q_{ij} > 0)$. The charge distribution function must select once for all one of the options once and then maintain this choice, to avoid the jumps that produce chattering and to limit the power required to perform the maneuver.

Three spacecraft optimal charge distribution

Let us consider a formation of three spacecraft, which will be labeled as *i*, *j*, *k*. As in the two spacecraft case, we look for the minimum charge distribution respecting two of the three constraints imposed by the controller.
The following cost function must be minimized:

$$V = \frac{1}{2}q_i^2 + \frac{1}{2}q_j^2 + \frac{1}{2}q_k^2 \tag{38}$$

together with two constraints on the charges. Without loss of generality we select the following two constraints:

$$Q_{ij} - q_i q_j = 0; \qquad Q_{jk} - q_j q_k = 0; \tag{39}$$

Such a choice imposes constraints on the virtual links joining the *i-th* with the *j-th* spacecraft and the *j-th* with the *k-th* spacecraft: it is the appropriate choice if the cost function E_{ki} is the minimum among the ones in Eq.(31), i.e. if the *i-th* and *k-th* spacecraft are the closest ones.
By introducing the Lagrange multipliers λ_{ij} and λ_{jk}, it is possible to add the constraints to Eq.(38), obtaining the following Hamiltonian function:

$$H = \frac{1}{2}q_i^2 + \frac{1}{2}q_j^2 + \frac{1}{2}q_k^2 + \lambda_{ij}\left[Q_{ij} - q_i q_j\right] + \lambda_{jk}\left[Q_{jk} - q_j q_k\right] \tag{40}$$

The necessary conditions for the optimality lead to the following system of equations:

$$\begin{aligned} &\frac{\partial H}{\partial q_i} = q_i - \lambda_{ij} q_j = 0 \qquad && \frac{\partial H}{\partial \lambda_{ij}} = Q_{ij} - q_i q_j = 0 \\ &\frac{\partial H}{\partial q_j} = q_j - \lambda_{ij} q_i - \lambda_{jk} q_k = 0 \qquad && \frac{\partial H}{\partial \lambda_{jk}} = Q_{jk} - q_j q_k = 0 \\ &\frac{\partial H}{\partial q_k} = q_k - \lambda_{jk} q_j = 0 \end{aligned} \tag{41}$$

After some algebra, the solution of the system of equation in Eq.(41) leads to the following relations:

$$\lambda_{ij} = \frac{q_i}{q_j} \qquad \lambda_{jk} = \frac{q_k}{q_j} \qquad q_i = \frac{Q_{ij}}{q_j} \qquad q_k = \frac{Q_{jk}}{q_j}$$
$$q_j^2 = q_i^2 + q_k^2 \tag{42}$$

that provide the following two real solutions, suitable for implementation:

$$\begin{aligned} &a) \quad q_j = \sqrt{Q_{ij}^2 + Q_{jk}^2} \qquad q_i = \frac{Q_{ij}}{\sqrt{Q_{ij}^2 + Q_{jk}^2}} \qquad q_k = \frac{Q_{jk}}{\sqrt{Q_{ij}^2 + Q_{jk}^2}} \\ &b) \quad q_j = -\sqrt{Q_{ij}^2 + Q_{jk}^2} \qquad q_i = -\frac{Q_{ij}}{\sqrt{Q_{ij}^2 + Q_{jk}^2}} \qquad q_k = -\frac{Q_{jk}}{\sqrt{Q_{ij}^2 + Q_{jk}^2}} \end{aligned} \tag{43}$$

As in the previous case, there is an indetermination about the sign of the charge to be associated on the *j-th* spacecraft. The other two cases, which take into account the other two combinations of the constraints, can be obtained by following the same procedure.

NUMERICAL RESULTS

Several numerical simulations have been performed in order to evaluate the effectiveness of the proposed control and charging strategies. The case of a formation of satellites in a GEO orbit ($r_R = 42000km$) is the selected scenario, because the Debye length in this orbit (which is generally included in the range $100m \le \lambda_d \le 1000m$, set to $\lambda_d = 100m$ in the tests) allows the success of formation acquisition and maintenance maneuvers with relatively low efforts in term of charge magnitudes.

The considered formation is composed by satellites having equal mass $(m_i = 500kg)$. The charge distribution is assumed to be uniform, under the hypothesis that the spacecraft can be considered spherically-shaped with a radius $R_i = 1\,m$. The charging capability of each satellite is limited by the maximum allowable currents ($i_{s+} = 1\mu A$ and $i_{s-} = -1\mu A$) and by the charge saturation limits ($q_{s+} = 50\mu C$ and $q_{s-} = -50\mu C$), corresponding to a spacecraft capacitance approximately equal to $C_i = 0.1\,pF$. Only electrostatic actions among the spacecraft are taken into account, and therefore not all the degrees of freedom of the system are controlled, leaving to further analysis the possibility to integrate this control methodology with other kind of propulsion.

The analysis involves the cases of two and three satellites formations and, starting from an initial inter-spacecraft distance d_{ij}^0, aims to the following mission goals:

- formation acquisition: to reach a desired distance d_{ij}^{des} between the spacecraft in a given maneuver time T_{acq}.
- formation maintenance: to maintain the desired distance d_{ij}^{des} between the spacecraft for an additional time period T_{mnt}.

Two spacecraft formation case

Initial positions and velocities with respect to the LVLH reference frame are $\vec{d}_1^{\,0} = [48.5, 8.5, 8.7]m$, $\vec{d}_2^{\,0} = [-48.5, -8.5, -8.7]m$, $\vec{V}_1^{\,0} = [0,0,0]m/s$ and $\vec{V}_2^{\,0} = [0,0,0]m/s$, corresponding to an initial distance $d_{12}^0 = 100\,m$, and the goal of the mission is to achieve a relative

distance of $d_{12}^{des} = 50m$ in $T_{acq} = 12h$ (half GEO orbit period) and to maintain this distance along an additional $T_{mnt} = 12h$. The Lyapunov based control in Eq.(22) is adopted first, with the gains $k_{12}^{p} = 3.0 \cdot 10^{-6}$ and $k_{12}^{d} = 3.0 \cdot 10^{-2}$, which have been selected by a trial-and-error process (an optimized procedure for gain selection is exposed in [20]). The path of the trajectories followed by the two spacecraft are represented in Figure 6, together with the distance vector joining them. Starting from their initial positions, the spacecraft approach each other by rapidly reducing their mutual distance till the desired value is reached, and then maintain the desired configuration until the end of the maneuver, as reported in Figure 7. It is clear that the virtual link between them begins to oscillate around the radial direction (as a rigid body under the gravity gradient actions). This special motion is due to the choice of particular initial condition and controller gains, which leads the system to remain near the stable position of the gravity gradient field.

The values of the charges needed to perform this maneuver are reported in Figure 8. It is worth to notice that the most demanding phase in terms of the spacecraft charge magnitudes is the acquisition, when the spacecraft have to be charged up to their saturation limits. Once the inter-spacecraft distance goal is almost achieved, the charges reduce to about $20\,\mu C$. The maintenance phase still needs a residual level of charges applied to the spacecraft (about $10\,\mu C$), because an electrostatic force will be needed to keep this configuration otherwise unattainable in free dynamics.

The required power, computed by means of Eq.(5), is surprising low: the largest needs in terms of power consumption are associated with the first hour of the maneuver when the spacecraft will charge in few minutes up to their saturation limits, to rapidly discharge themselves later as soon as the distance is remarkably reduced. On the other hand, for the formation maintenance phase the needs in power are very low, as shown in the bottom plot of Figure 9, and related to the charge modulation already visible in Figure 8: only $23.5\,J$ energy are required to perform the entire maneuver.

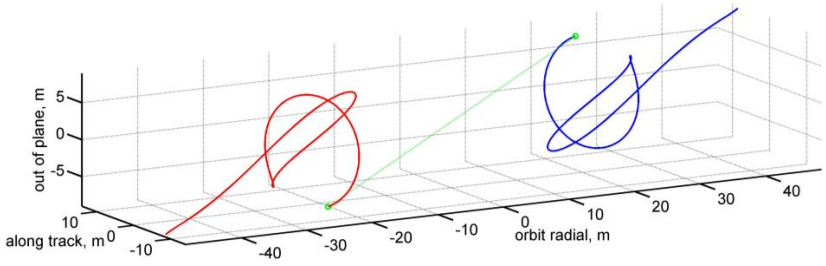

Figure 6. Path of trajectories of the two spacecraft librating formation

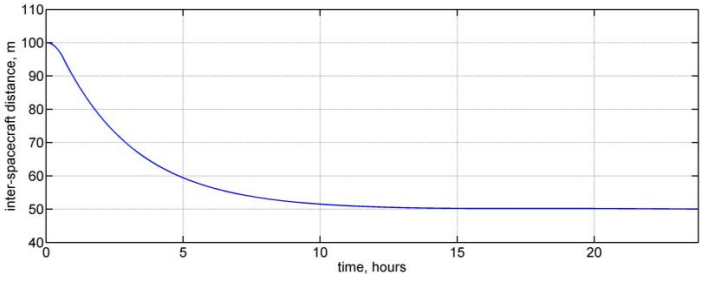

Figure 7 Inter-spacecraft distance for the two spacecraft librating formation

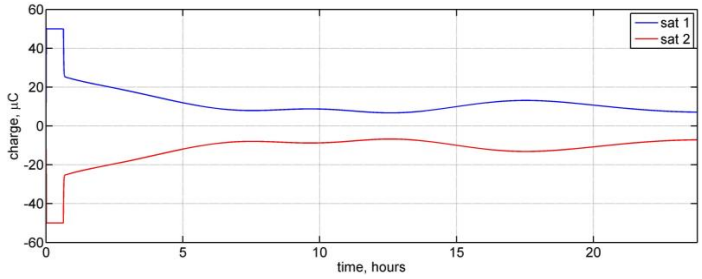

Figure 8. Spacecraft charges for the two spacecraft librating formation

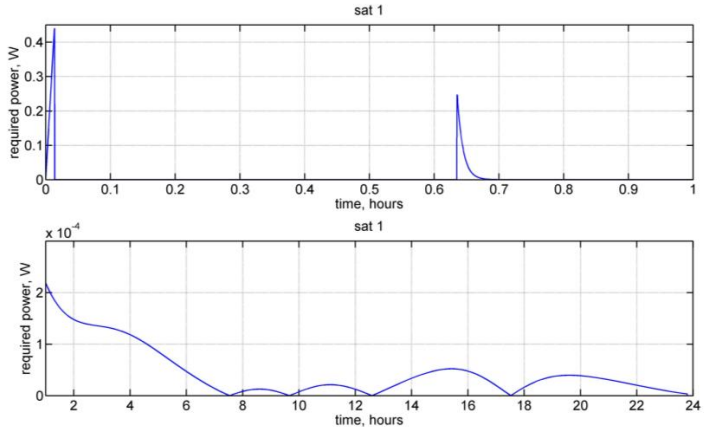

Figure 9. Required power for two spacecraft librating formation

The specific configuration obtained is one among several possibilities for a two spacecraft formation. In fact, different gains of the controller will generate a different behavior, even starting from the same set of initial conditions and targeting the very same mission requirements. The trajectories corresponding to the gains $k_{12}^{p} = 5.0 \cdot 10^{-6}$ and $k_{12}^{d} = 1.0 \cdot 10^{-2}$ are represented in Figure 10 with the two spacecraft that, after a sudden approach, begin to rotate with respect the center of mass of the entire system. The relevant behavior of the charges is shown in Figure 11, where it is possible to notice that after the saturation phase (which produces an attractive force) the second satellite changes the sign of its charge to create a repulsive action. The steady state is reached before the required $T_{acq} = 12\,h$ and the charges are slightly modulated to counteract the variable inertial actions. The effects of the centrifugal actions are also present in Figure 12, where the distance between the two spacecraft approaches rapidly the desired value without actually reaching it. The steady state error can be explained as the controller is not designed to tackle centrifugal actions. The same rotating behavior can be obtained as an example by the SDRE control, with the following gain matrices (see Eq.(24)): $\mathbf{Q} = \mathrm{diag}\left([k_{12}^{p}, k_{12}^{d}]\right)$ and $\mathbf{R} = k_{12}^{u}$, with $k_{12}^{p} = 10^{-8}$, $k_{12}^{d} = 10^{-6}$, $k_{12}^{u} = 10^{+12}$ (plots not reported). The energy required amounts to $29.7\,J$ for the SDRE case and $14.7\,J$ for the Lyapunov based control (values referred to each single spacecraft).

In order to reduce the steady state error it is possible to add to the controller an integral term, as done in the Eq.(23) with the gain $k_{12}^{i} = 10^{-10}$. Such a choice is successful as shown in Figure 13,

even if it does involve several changes in the sign of the charge of the second spacecraft (Figure 14).

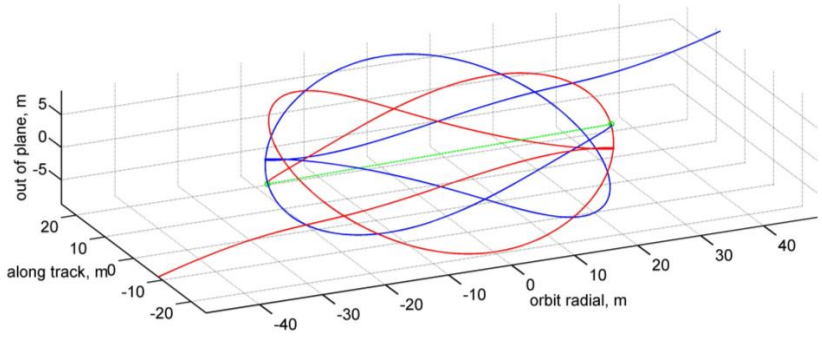

Figure 10. Path of the trajectories of the two spacecraft rotating formation

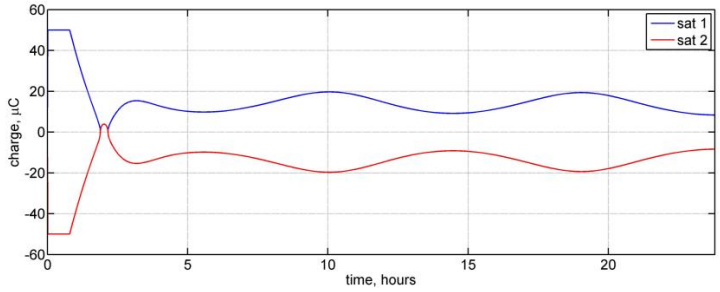

Figure 11. Charge distribution during the rotating formation case (Lyap+PD)

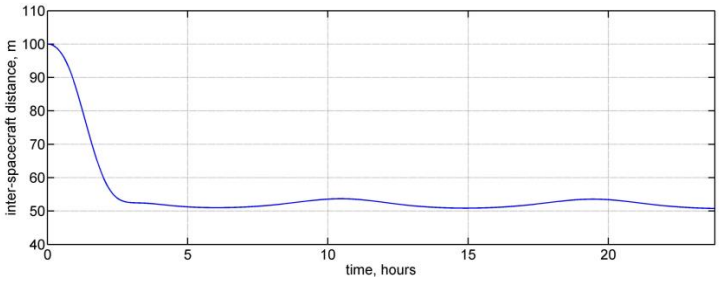

Figure 12. Inter-spacecraft distance during the rotating formation case (Lyap+PD)

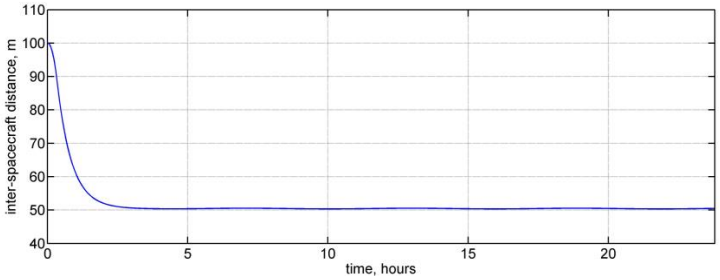

Figure 13. Inter-spacecraft distance during the rotating formation case (Lyap+PID)

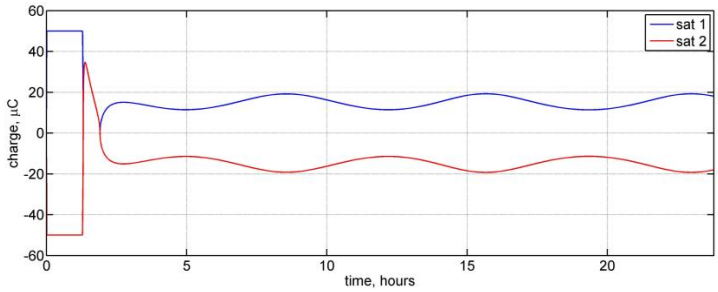

Figure 14. Charge distribution during the rotating formation case (Lyap+PID)

Three spacecraft formation case

The scenario consists of three spacecraft whose initial positions and velocities with respect to the LVLH reference frame are $\vec{d}_1^0 = [-50.0, -28.9, 0.0]m$, $\vec{d}_2^0 = [50.0, -28.9, 0.0]m$, $\vec{d}_3^0 = [0.0, 57.7, 0.0]\,m$, $\vec{V}_1^0 = [0,0,0]m/s$, $\vec{V}_2^0 = [0,0,0]m/s$ and $\vec{V}_3^0 = [0,0,0]m/s$, with starting distances among the spacecraft $d_{12}^0 = d_{23}^0 = d_{31}^0 = 100\,m$, corresponding to an equilateral triangle shape. The goal of the mission is to reduce these distances to $d_{12}^{des} = d_{23}^{des} = d_{31}^{des} = 50m$ in half GEO orbit period ($T_{acq} = 12h$) and to maintain them during an additional time interval $T_{mnt} = 12h$. As previously discussed, it is impossible to simultaneously reduce the lengths of all the links. A suitable control strategy is represented in Figure 4: this scheme takes into account the solutions given by the global controllers (Lyapunov or SDRE) and selects to chase, by means of the evaluation of the error functions in Eq.(31), only two out of the three products of charges. The periodic switch among these constraints ensures the convergence. The switching time interval Δt_{sw} becomes the key parameter, to be selected in order to trade-off between two opposite goals: Δt_{sw} cannot be too small in order to limit the chattering phenomena, nor too large in order to avoid that the uncontrolled virtual link of the formation remains uncorrected during the next switch phase. In particular the effects of three different switching periods ($\Delta t_{sw} = 1\min, 10\min, 30\min$) are analyzed.

In Figure 15 the evolution of the formation for the $\Delta t_{sw} = 30\min$ case is represented, with the corresponding trends of the cost functions (Eq.(31)) reported in Figure 16. A pseudo-steady trend will be achieved after about 6 hours (see Figure 17), approaching the desired value of the inter-satellite distances with a remaining, limited chatter due to the continuous switching. The inversions in charges' sign are easily noticeable in Figure 18, together with the saturation bounds' effects. Figure 19, where spikes of $\pm 1\mu A$ appear periodically at every switch, plots the relevant currents. As a result, also the required power has an impulsive envelope, as shown in Figure 20.

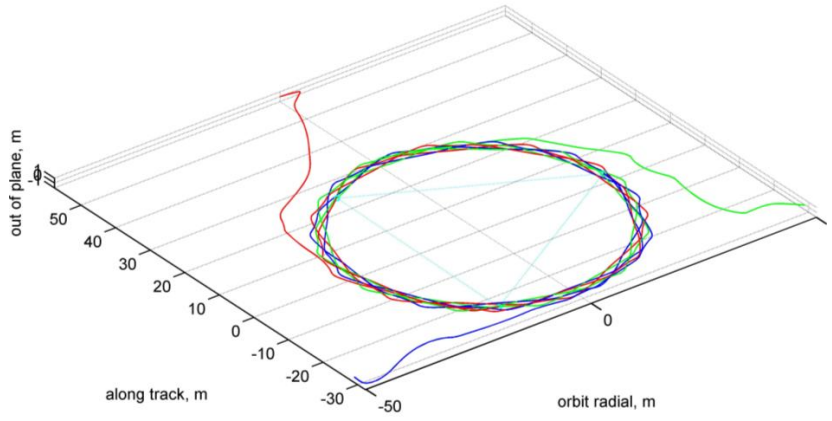

Figure 15. Paths of the trajectories for the three spacecraft maneuver ($\Delta t_{sw} = 30\,\mathrm{min}$)

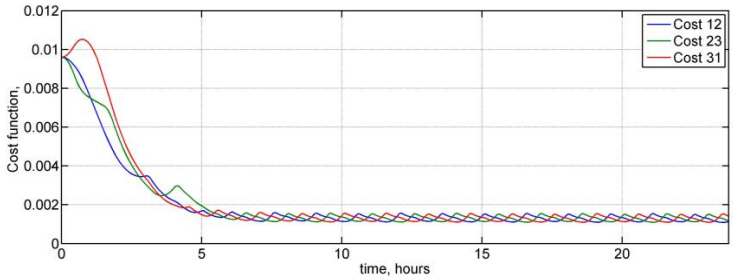

Figure 16. Cost functions of the switching strategy

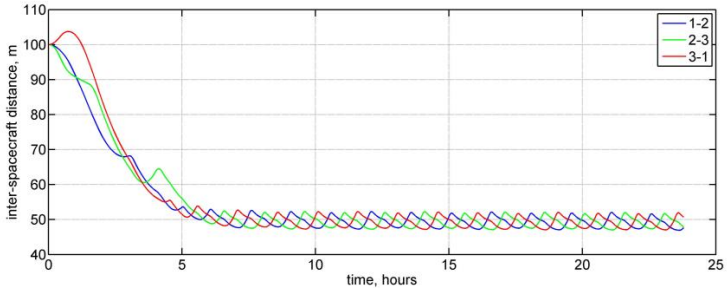

Figure 17. Distances among the spacecraft during the acquisition maneuver

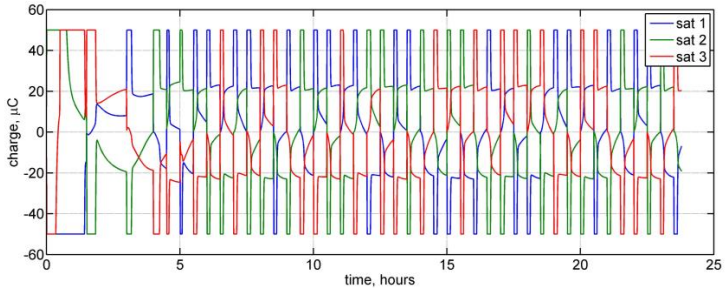

Figure 18. Charges during the acquisition maneuver of three spacecraft formation

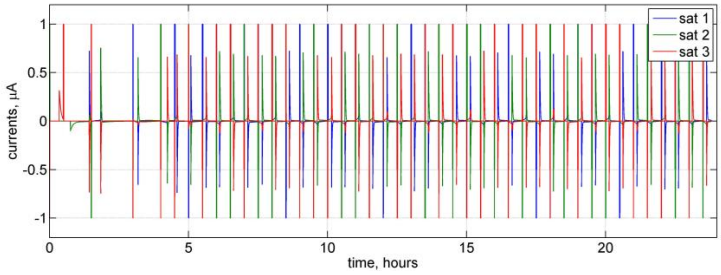

Figure 19. Ion/electron fluxes during the acquisition maneuver.

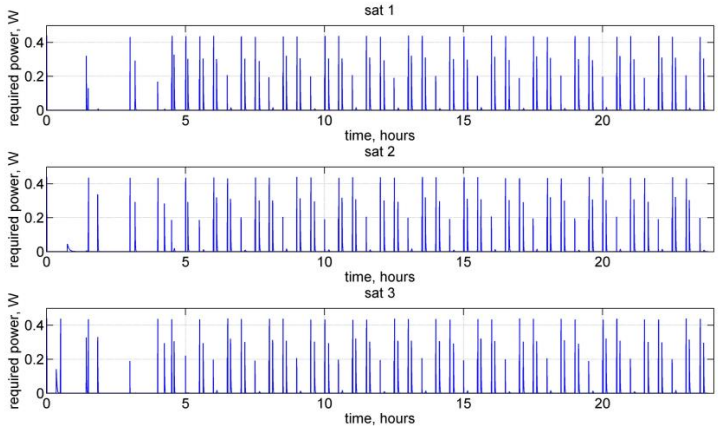

Figure 20. Required power for the three spacecraft acquisition maneuver

Two other switching intervals have been considered. Figure 21 reports the trajectories during the acquisition maneuver corresponding to $\Delta t_{sw} = 10\,\text{min}$. It is worth to notice that the paths are now smoother, as the uncontrolled side of the triangle has a shorter time to degenerate, and the deviations from the nominal value are therefore smaller in magnitude with respect to the previous case. On the other hand the acquisition maneuver (obtained with the same gains) takes a time longer than before (see Figure 22), requiring all the 12 hours devoted to this phase. In Figure 22 a remarkable reduction of the chattering is also visible and the formation maintains itself close to the desired configuration. These better results are paid in terms of required rapidly in charge

changing, leading to higher power/energy needs to perform the maneuver, as proofed by Figure 23.

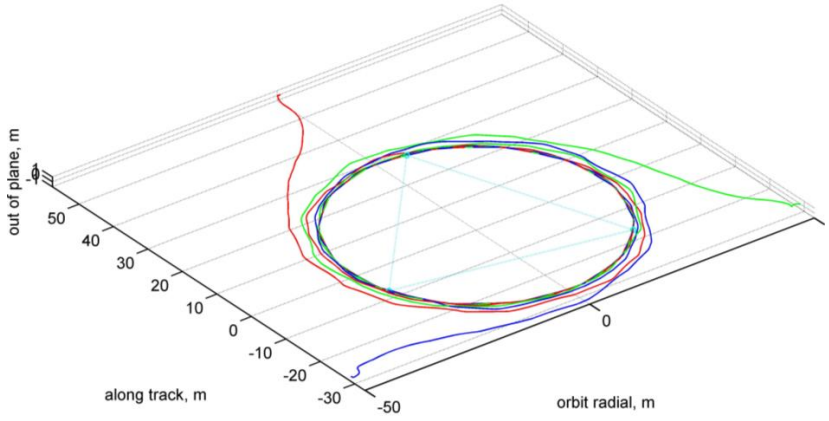

Figure 21. Paths of the trajectories for the three spacecraft maneuver ($\Delta t_{sw} = 10\,\mathrm{min}$)

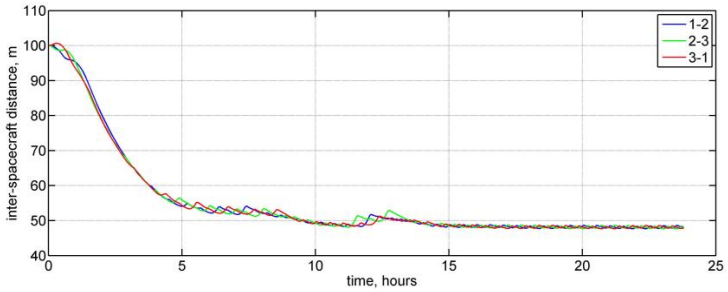

Figure 22. Distances among the spacecraft during the acquisition maneuver ($\Delta t_{sw} = 10\,\mathrm{min}$)

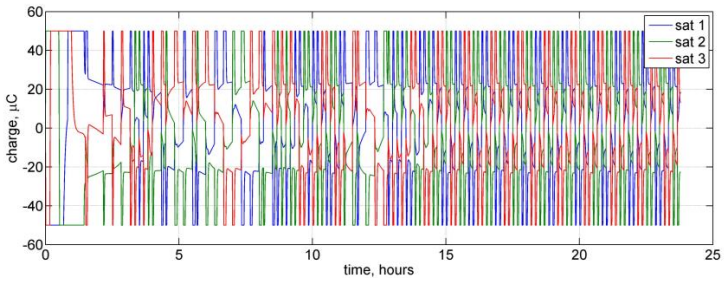

Figure 23. Charges during the acquisition maneuver ($\Delta t_{sw} = 10\,\mathrm{min}$)

The best result, in terms of a smooth behavior, has been obtained with the switch interval $\Delta t_{sw} = 1\,\mathrm{min}$. Relevant spacecraft trajectories are reported in Figure 24, where the edges which characterized the previous cases disappear. The same regular behavior is present in Figure 25, where the inter-spacecraft distances are plotted, and the three sides of the triangle configuration can be seen reducing almost simultaneously their length. This performance is paid in terms in

energy consumption, as reported in Table 1: the cost increases as the switching period decreases, due to the frequent, sudden variation in currents.

The analysis shows how the electrostatic control can be applied with reasonable efforts in terms of power and energy, especially if the requirements in distances are of the order of the meter. It is also clear that if the strategy easily fits strict requirements on the inter-satellite distances' accuracy.

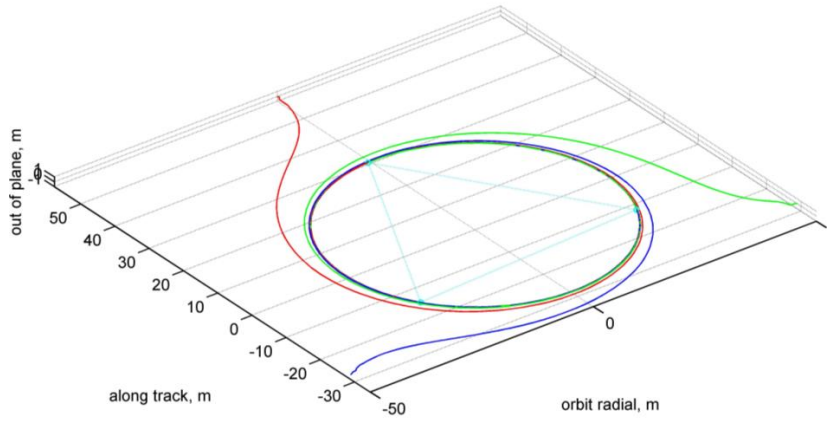

Figure 24. Paths of the trajectories for the three spacecraft maneuver ($\Delta t_{sw} = 1\,\mathrm{min}$)

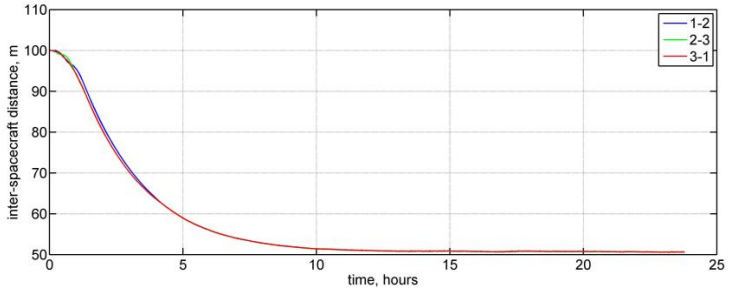

Figure 25. Distances among the spacecraft during the acquisition maneuver($\Delta t_{sw} = 1\,\mathrm{min}$)

Table 1 Energy consumptions

Switching time	Satellite 1	Satellite 2	Satellite 3
30 min	685.9 J	691.6 J	707.8 J
10 min	1801.4 J	1777.3 J	1739.9 J
1 min	5836.0 J	5777.6 J	6091.9 J

CONCLUSIONS

The electrostatic control of the spacecraft formations' configuration, obtained by means of purposeful satellite surface charging, is a technique facing increasing interest, with the significant advantage of a quite high precision at a moderate cost. Analysis and simulations are currently developed to better understand the suitability of this concept. This paper presents a model that includes important constraints as the saturation limits on maximum allowable currents and the maximum values for spacecraft charging. This model is used to analyze the control strategies in the cases of two and three spacecraft formations in GEO. A reduced set of equation of motion is obtained first, to pave the way to apply and compare two global control strategies (Lyapunov-based control and SDRE-based control). The computed control actions are provided in terms of spacecraft charge products, requiring an additional step to actually identify a suitable distribution of the charges among the spacecraft. The two spacecraft formation simulations highlighted the characteristics of the electrostatic control, showing that the power/energy consumption is strictly connected to the changes in charges required for performing the maneuvers. A surprising result of the Coulomb interaction study is that the magnitude of the inter-spacecraft forces is comparable with the one provided by micro-propulsion systems proposed for formation keeping.

The main result of this work deals with the three spacecraft formation analysis. A preliminary analysis of the three spacecraft problem proofed as the partition of the charge products obtained as output from the controllers is far from trivial. To overcome such an issue, a switching strategy has been selected in order to satisfy only a subset - to be periodically exchanged - of the requirements. Numerical results showed the strictly dependence of the precision of the inter-spacecraft distance on the duration of the switching period: specifically, the smaller the switching interval, the more precise will be the acquisition of the targeted configuration, at the cost of higher energy consumption and power requirement.

Overall, the resulting energy values, even if quite preliminary, show that electrostatic control could be usefully applied, especially if the requirements in distances are of the order of tens of meters. Advantages as the precision and the lack of plume impingement effects add important value and suggest further investigations.

REFERENCES

[1] King, L.B., Parker, G.G, Deshmukh, S., Chong, J.H., "A study of Inter-Spacecraft Coulomb Forces and Implications for Formation Flying", paper AIAA 2002-3671, *38th AIAA/ASME/SAE/ASEE Joint Propulsion Conference and Exhibit* (2002).

[2] King, L.B., Parker, G.G, Deshmukh, S., Chong, J.H., "Spacecraft Formation-Flying using Inter-Vehicle Coulomb Forces", *NASA/NIAC Tech. Rep*., Jan. 2002.

[3] Pettazzi, L., Kruger, H., and Theil, S., "Electrostatic Forces for Satellite Swarm Navigation and Reconfiguration", *ESA/ACT, Ariadna Final Report (05-4107a)*, 2006.

[4] Saaj, C.M., Lappas, V., Richie, D., Peck, M., Streetman, B., and Schaub, H., "Electrostatic Forces for Satellite Swarm Navigation and Reconfiguration", *ESA/ACT Ariadna Final Report (05-4107b)*, 2006.

[5] Schaub, H., Parker, G.G, King, L.B., "Challenges and Prospects of Coulomb Spacecraft Formations", *AAS John L. Junkins Symposium,* College Station, TX, May 22-23 2003, AAS 03-278.

[6] Jones, D. R, Schaub, H., "Optimal reconfigurations of two-craft Coulomb formations along manifolds", *Acta Astronautica*, Volume 83, Feb.–Mar. 2013, pp. 108-118.

[7] Inampudi R., Schaub. H., "Optimal Reconfigurations of Two-Craft Coulomb Formation in Circular Orbits", *Journal of Guidance, Control, and Dynamics*, Vol. 35, No. 6 (2012), pp. 1805-1815.

[8] Hogan, E. A., Schaub, H., "Relative Motion Control For Two-Spacecraft Electrostatic Orbit Corrections", *Journal of Guidance, Control, and Dynamics*, Vol. 36, No. 1 (2013), pp. 240-249.

[9] Wang, S., Schaub, H., "Coulomb Control of Non-equilibrium Fixed Shape Triangular Three-Vehicle Cluster", *Journal of Guidance, Control, and Dynamics*, Vol. 34, No. 1 (2011), pp. 259-270.

[10] Wang, S.; Schaub, H., "One-Dimensional Constrained Coulomb Structure Control with Charge Saturation,", *IEEE Transactions on Aerospace and Electronic Systems*, vol.48, no.1 (2012), pp.3-15.

[11] Wang S., Schaub. H., "Nonlinear Charge Control for a Collinear Fixed-Shape Three-Craft Equilibrium", *Journal of Guidance, Control, and Dynamics*, Vol. 34, No. 2 (2011), pp. 359-366.

[12] Schaub. H., "Stabilization of Satellite Motion Relative to a Coulomb Spacecraft Formation", *Journal of Guidance, Control, and Dynamic*s, Vol. 28, No. 6 (2005), pp. 1231-1239.

[13] Kamhawi, H., Patterson, M., and Dalton, P., "Operational Status of the International Space Station Plasma Contactor Hollow Cathode Assemblies", paper AIAA 2011-5990, *47th AIAA/ASME/SAE/ASEE Joint Propulsion Conference & Exhibit*, (2011).

[14] Goebel, D. M., Kats, I., "Fundamentals of Electric Propulsion: Ion and Hall Thrusters", *JPL Space Science and Technology Series*, John Wiley & Sons, 2008

[15] Mullen, E.G., Gussenhoven, M.S., Hardy, D.A, Aggson, T.A., Ledley, B.G., Whipple, E., "SCATHA survey of high level spacecraft charging in sunlight", *Journal of Geophysical Research: Space Physics*, Vol. 91, A2, pp. 1474-1490 (1981).

[16] R.C. Olsen, C.E. McIlwain, E.C. Whipple, "Observations of differential charging effects on ATS 6", *Journal of Geophysical Research: Space Physics*, Vol. 86, A8, pp. 6809-6819 (1981).

[17] Clohessy,W., Wiltshire, R., "Terminal guidance system for satellite rendezvous", *Journal Aerospace Science*, Vol. 27, pp. 653-658 (1960).

[18] Felicetti, L.; Palmerini, G.B., "Modeling the formationkeeping control with multibody codes," *IEEE Aerospace Conference Proceedings* (2012), doi: 10.1109/AERO.2012.6187070

[19] Felicetti, L., Palmerini, G.B. "Formation flying dynamics analysis by means of a virtual multibody approach", *Advances in the Astronautical Sciences*, vol. 145 (2012), pp. 577-596.

[20] Felicetti, L., Palmerini, G.B., "Evaluation of Control Strategies for Spacecraft Electrostatic Formation Keeping", *IEEE Aerospace Conference Proceedings* (2014).

[21] Palmerini, G.B., "Guidance Strategies for Satellite Formations", *Advances in the Astronautical Sciences*, Vol. 103, (2000), pp. 135-145.

[22] Beeler, S.C.,"State-Dependent Riccati Equation Regulation of Systems with State and Control Nonlinearities", *NASA/CR-2004-213245*, NIA Report No. 2004-08 (2004).

[23] H.T., Banks, B.M. Lewis, H.T. Tran, "Nonlinear Feedback Controllers and Compensators: A State-Dependent Riccati Equation Approach", *Computational Optimization and Applications*, vol.37, No.2 (2007), pp. 177-218.

[24] Cimen, T., "State-Dependent Riccati Equation (SDRE) Control: A Survey", *Proceedings of the 17th World Congress International Federation of Automatic Control*, Seoul (2008).

[25] Felicetti, L., Palmerini, G. B., "A comparison among classical and SDRE techniques in formation flying orbital control", *IEEE Aerospace Conference Proceedings* (2013), doi: 10.1109/AERO.2013.6497414

[26] Luenberger, D.G., "Linear and Nonlinear Programming", 2nd ed., Addison-Wesley., 1984.